Thermophysical and Spectral Variability of Arsia Mons Lava Flows

Michael Ramsey: Dept. of Geology & Planetary Science, University of Pittsburgh, Pittsburgh, PA; mramsey@pitt.edu

David Crown: Planetary Science Institute, Tucson, AZ; crown@psi.edu

INTRODUCTION:

Arsia Mons (9.5°S, 239.5°E) is the southernmost of the Tharsis shield volcanoes and the second largest volcano by volume on Mars. It is more than 9 km higher than the surrounding plains with a well-developed summit caldera [1-3]. Two large aprons of lava flows on the NE and SW flanks extend from alcoves in the caldera wall and post-date the main shield-forming stage [4-5]. The SW apron has an average slope of 0.6° with a well-developed flow field [4]. The flows exhibit a wide range of flow surfaces, textures, and degrees of eolian mantling [6-7].

The research here focuses on a series of lava flows (22.5° S, 238.0°E), which have a multitude of textures and unusual thermophyscial characteristics (Figure 1). The local slopes in this region are less than 0.3°; however the small-scale RMS roughness has been modeled using the thermal infrared (IR) emissivity spectra to be as large 15° [8]. Our past studies have utilized the Mars Odyssey (MO) Thermal Emission Imaging System (THEMIS) visible camera (VIS), the Mars Reconnaissance Orbiter (MRO) Context Camera (CTX) and High Resolution Imaging Science Experiment (HiRISE) to examine the small-scale development of channel and levee systems as well as the degree of mantling [6]. This work now incorporates data from the THEMIS IR system to extract the surface composition and textural variability of these flows.

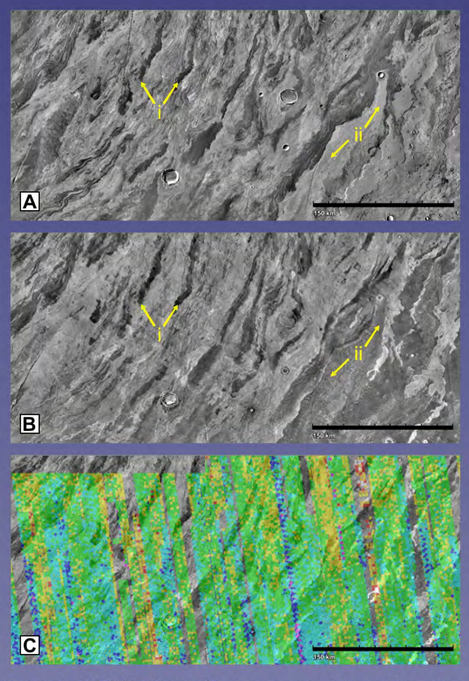

Figure 1: THEMIS infrared (IR) data mosaic of the southern Arsia Mons flow field showing the distinct thermophysical variations. **(A)** Daytime IR mosaic. **(B)** Nighttime IR mosaic. Note certain flows do not exhibit significant changes in thermal radiance between day and night (i), whereas others have a distinct day/night thermal variation (ii). **(C)** TES-derived dust cover index (DCI) of the region. The colors represent a variation of between 0.95 – 0.97 and the TES-derived albedo for the region varies between 0.24 – 0.26.

FLOW FIELD MAPPING:

Flow field maps show small vents, channels, and distinct flow lobe margins (Figure 2). Morphometric parameters (e.g., length, width, thickness, sinuosity, etc.) for individual flow lobes were used to document the development of channel and levee systems as well as provide a general characterization of flow field properties and emplacement over different slopes [7]. These images revealed small-scale characteristics of the lava flow surfaces and new insights into flow emplacement processes, useful for understanding the styles and diversity of volcanism [6-7,9]. HiRISE images also provided cm-scale characterizations to derive the percentage of exposed bedrock and mantling deposits, the occurrence of boulders, and the abundance and preservation states of small impact craters.

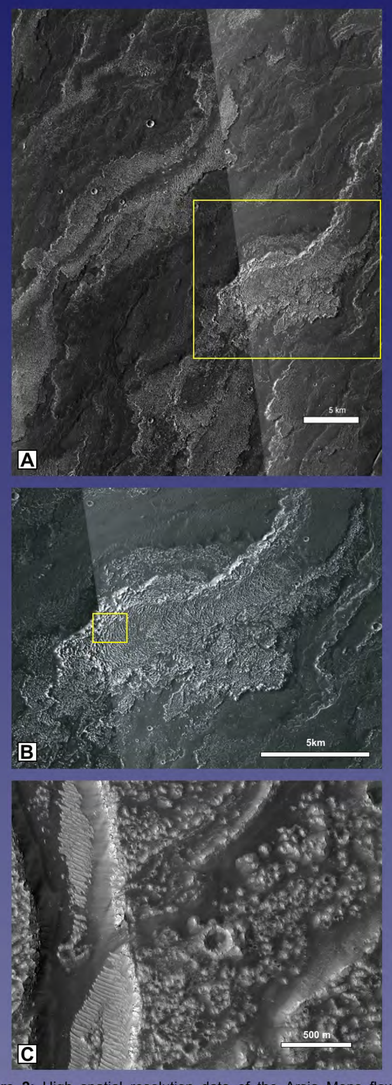

Figure 2: High spatial resolution data of the Arsia Mons flow field centered at 121.50°W, 22.13°S showing the complex flow relationships [e.g., 7] and different flow morphologies (i.e., bright/rugged and dark/smooth). **(A)** CTX data mosaic with yellow box indicating the area shown in (B). **(B)** Full resolution CTX image mosaic with yellow box indicating the area shown in (C). **(C)** HiRISE image (PSP_006614_1580) showing the lower albedo mantling of the higher albedo lava flow surface. This mantling material covers ~ 50% of the flow surface [6].

THEMIS DATA:

The thermal IR imager on THEMIS consists of an array of uncooled microbolometer detectors with 10 spectral channels centered between 6.76 and 14.8 µm with a spatial resolution of 100 m [10-11]. The first two channels are duplicated for better signal to noise and the tenth channel is used to determine atmospheric opacity [10]. The IR data presented here (I07370003) were acquired with all 10 bands at Ls = 240 and a local solar time of 17:06:11. The data were atmospherically-corrected using previously-collected data from the Thermal Emission Spectrometer (TES) and separated into brightness temperature and apparent surface emissivity [11]. The derived scene temperatures ranged from 240 to 283 K with a maximum dust opacity of 0.34.

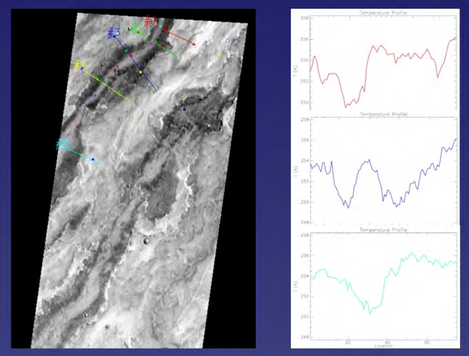

Figure 3: THEMIS-derived temperature data (I07370003) following atmospheric correction using TES data [11]. Colored lines correspond to the temperature profiles at right. Distinctly warmer center channels of the rugged flows indicate higher amounts of eolian mantling.

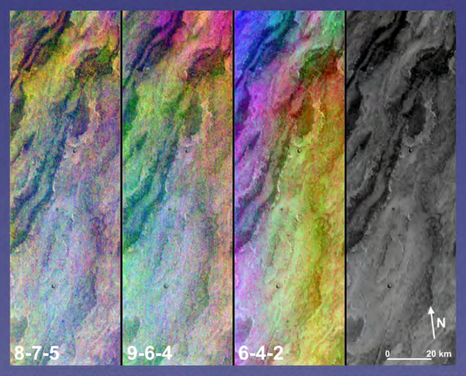

Figure 4: THEMIS DCS and brightness temperature images. The subtle yet distinct colors of the flows indicate TIR spectral diversity.

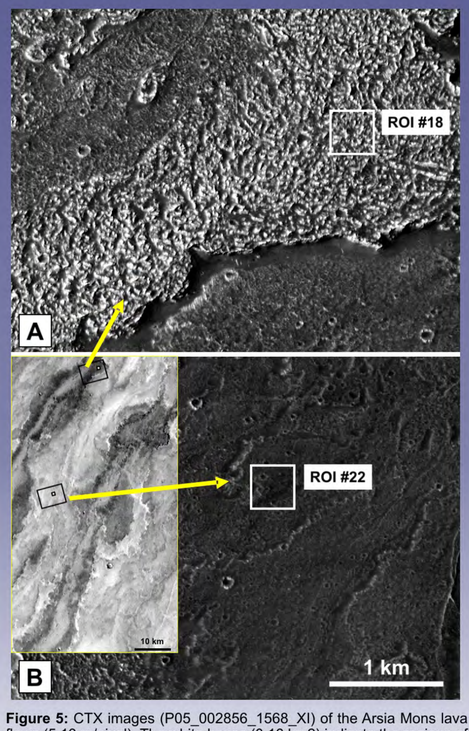

Figure 5: CTX images (P05_002856_1568_XI) of the Arsia Mons lava flows (5.13 m/pixel). The white boxes (0.16 km2) indicate the regions of interest (ROI) from which the THEMIS IR spectra were extracted (Figure 7). Inset is a THEMIS daytime temperature context image (I07370003). The lower temperatures (darker surfaces) correspond to the rugged levees of the higher (visible) albedo flows. **(A)** Higher albedo flow with rugged levees. **(B)** Lower albedo flow fields containing narrow channels and diffuse terminations.

RESULTS:

Rugged levees commonly have daytime temperatures ~4° lower than the warmer channels and the surrounding lower albedo flows, indicating a higher thermal inertia (Figure 3). The TES-derived albedo and dust cover index predict moderate levels of dust cover for the region [12]. Some flows show no temperature inversion between day and night IR data, which is likely the result of an albedo-dominated influence of radiant temperature. Typically, such regions are not conducive for surface emissivity analysis; however, the thermophysical diversity and lower dust cover on some flows warranted the further examination presented here.

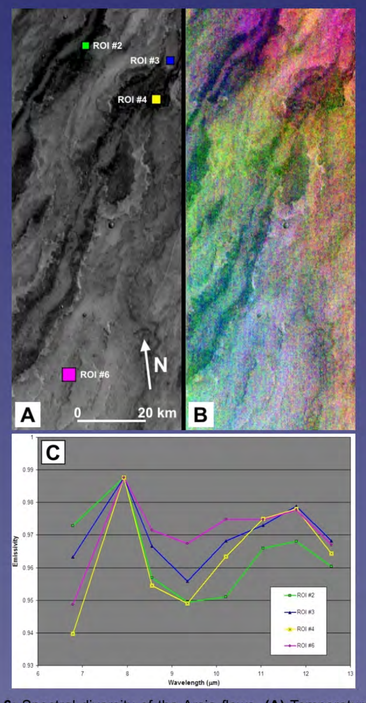

Figure 6: Spectral diversity of the Arsia flows. **(A)** Temperature image with the locations and sizes of four ROIs. ROI #2 and #4 were extracted from the more rugged (cooler) flows, whereas ROI #1 and #4 were from the lower albedo smoother flows. **(B)** Corresponding 9-6-4 DCS image. **(C)** Spectra from the ROIs that show the shorter wavelength absorption of ROIs #2 and #4 perhaps indicating a less mafic composition.

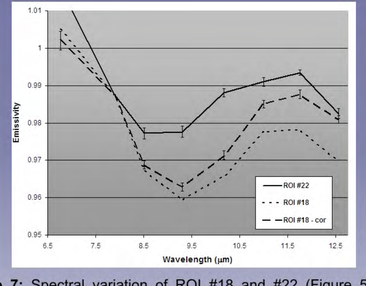

Figure 7: Spectral variation of ROI #18 and #22 (Figure 5). The spectrum of the rugged flows shows a distinct long wavelength slope commonly seen on surfaces with thermal heterogeneities [11]. After the distortion has been removed the spectra are still distinct indicating slightly different compositions. It is expected that these differences would be even more pronounced once the spectral overprinting of the eolian mantling on the rugged units has been removed.

Regions of interest (ROIs) were extracted over 16 THEMIS IR pixels in 26 different locations. These were chosen to compare the: 1) rugged and smooth flows (Figure 6) and 2) down flow changes (Figure 8). Emissivity spectra from these ROIs contained significant diversity. The smoother flows had spectra that were ~50% shallower with the strongest absorption at 9.3 µm, whereas the rougher *(less mafic?)* flows commonly had an absorption at 8.5 µm. The rugged flow spectra also had a negative slope toward longer wavelengths, evidence of subpixel thermal heterogeneity due to significant surface roughness [8]. These spectra were corrected using a simple linear slope fitting approach (Figure 7). The observed spectral differences do not appear to be a linear combination of the two flow type spectral end-members. The morphological and spectral differences likely indicate different emplacement histories and possibly compositions.

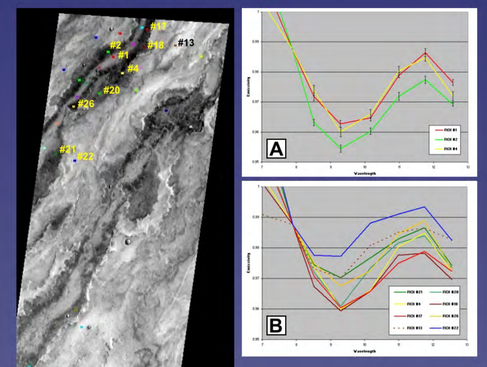

Figure 8. Spectral variation across the levee/channel **(A)** and down flow **(B)**. ROIs #4, #17 and #18 were extracted from rugged levees further upflow than #20, #21 and #26. The former have absorptions at longer wavelengths indicating a down-flow change in composition or the degree of eolian mantling.

Figure 9: Examples of rugged flow levees later filled with smoother pahoehoe flows (Mauna Ulu flow field, Kilauea, Hawaii). Similar flow processes can be seen on a larger scale at the Arsia flows coupled with some level of eolian mantling.

REFERENCES:

[1] Crumpler, L.S. et al. (1996), Geol. Soc. Spec. Publ., 110, 307-348.
[2] Head, J.W. et al. (1998), LPSC XXIX, abs. 1488.
[3] Mouginis-Mark, P.J. (2002), Geophys. Res. Lett., 29, 1768, doi:10.1029/2002GL015296.
[4] Plescia, J.B. (2004), J. Geophys. Res., 109, E03003, doi:10.1029/2002JE002031.
[5] Scott, D.H. and J.R. Zimbelman (1995), U.S. Geol. Surv. Misc. Invest. Ser. Map I-2480.
[6] Crown, D.A. et al. (2009), LPSC XL, abs. 1488.
[7] Crown, D.A. et al. (2010), LPSC XLI, abs. 2225.
[8] Bandfield, J.L. (2009), Icarus, 202, 414-428.
[9] Bleacher, J.E. et al. (2007), J. Geophys. Res., 112, E09005, doi:10.1029/2006JE002873.
[10] Christensen, P.R. et al. (2004), Space Sci. Rev., 110, 85-130.
[11] Bandfield, J.L. et al. (2004), J. Geophys. Res., 109, 10.1029/2004JE002289.
[12] Ruff, S.W. and P.R. Christensen (2002), J. Geophys. Res., 107, 5127, doi:10.1029/2001JE001580.